Identification of Androgen Receptor Variant 7-related RNAs Affecting Abiraterone Efficacy in Castration-resistant Prostate Cancer Treatment by RNA-sequencing

Shuo Wang
Key Laboratory of Carcinogenesis and Translational Research(Ministry of education/Beijing), Peking University Cancer Hospital and Institute

Yudong Cao
Key Laboratory of Caicinogenesis and Translational Research(Ministry of education/Beijing), Peking University Cancer Hospital and Institute

Xingxing Tang
Key Laboratory of Caicinogenesis and Translational Research(Ministry of education/Beijing), Peking University Cancer Hospital and Institute

Yong Yang
Key Laboratory of Carcinogenesis and Translational Research(Ministry of education/Beijing), Peking University Cancer Hospital and Institute

Peng Du (dupeng9000@126.com)
Key laboratory of carcinogenesis and translational research(Ministry of education/Beijing), Peking University Hospital and Institute

Research article

Keywords: Abiraterone, androgen receptor, bioinformatics analyses, castration resistance, prostate cancer, RNA-sequencing

Posted Date: October 29th, 2020

DOI: https://doi.org/10.21203/rs.3.rs-97303/v1

Abstract

Background: This study aimed to identify androgen receptor variant 7 (AR-V7)-related RNAs affecting Abiraterone treatment of castration-resistant prostate cancer (CRPC) using RNA-sequencing**.**

Methods: To identify AR-V7-related RNAs affecting Abiraterone treatment of CRPC, a series of *in vitro* experiments were employed, including cell proliferation assay, cell apoptosis assay, Western blot analysis, and Real-time quantitative reverse transcription PCR (qRT-PCR). After RNA-sequencing, the differentially expressed (DE) mRNAs and DE long non-coding RNAs (lncRNAs) were screened and the lncRNA-mRNA pairs were identified. In addition, enrichment and Protein-protein interaction (PPI) network analyses were performed. Finally, the mRNA-miRNA-lncRNA competing endogenous RNAs (ceRNA) network was built, along with survival analysis.

Results: A total of 1,387 AR-V7-related RNAs affecting Abiraterone treatment of CRPC were identified. The enrichment analysis showed that the target genes of DEmRNAs and DElncRNAs were primarily involved in cancer-related pathways, including the ErbB signaling pathway, pathways in cancer, and basal cell carcinoma. In addition, notch receptor 1 (NOTCH1), ionotropic NMDA glutamate receptor type subunit 1 (GRIN1), U-box containing protein 1 (STUB1), and mitogen-activated protein kinase 7 (MAP2K7) with high degrees in the PPI network. Moreover, MAP2K7 was regulated by hsa-miR-6825-5p, which in turn was regulated by MAFG-AS1 lncRNA in the ceRNA network. The survival analysis revealed that a total of four lncRNAs, including MAFG-AS1, and 17 mRNAs, including high muscle blind-like splicing regulator 2 (MBNL2), were associated with disease-free survival (RFS). Among them, only MBNL2 overexpression correlated with good survival outcome. The NOTCH1, GRIN1, STUB1, MBNL2, and ErbB signaling pathways are likely related to the efficacy of Abiraterone in CRPC treatment. Moreover, the MAFG-AS1-hsa-miR-6825-5p-MAP2K7 axis could be a therapeutic target for Abiraterone in CRPC treatment.

Conclusions: NOTCH1, GRIN1, STUB1, MBNL2, and the ErbB signaling pathway may relate to the progression of CRPC. MAFG-AS1-hsa-miR-6825-5p-MAP2K7 axis might be a potential therapeutic target for Abiraterone in CRPC.

Highlights

1. Abiraterone administration reduced *in vitro* AR-V7 expression.
2. A total of 1,387 AR-V7-related RNAs affected Abiraterone treatment of CRPC.
3. Only MBNL2 overexpression revealed good survival outcomes.
4. NOTCH1, GRIN1, STUB1, MAP2K7 with high degrees in the PPI network.
5. We provide new options for Abiraterone treatment of CRPC.

Background

Prostate cancer (PCa), the most common malignancy in men, had a global incidence rate that was second only to lung cancer in 2018 [1]. With changes in lifestyle and diet, as well as an aging population, the incidence of PCa in China is increasing every year [2]. Androgen deprivation therapy (ADT) achieves prostate-specific antigen (PSA) rate decline or disease control in patients with advanced PCa [3]. However, almost all PCa patients progress to castration-resistant prostate cancer (CRPC) after a period of treatment. Thus, it is urgent to understand the specific molecular mechanism of CRPC progression and search for potential therapeutic targets for CRPC.

The androgen receptor (AR) plays a key role in the progression of CRPC. CRPC invariably develops due to the aberrant reactivation of the androgen/AR signaling axis [4]. In addition, the expression levels of AR splice variants (AR-Vs) in CRPC were generally higher than those in hormone-naive PCa, especially AR-V7 (also known as AR3) and AR^{v567es} [5]. Numerous studies show that AR-V7 is associated with the development of CRPC [6–8]. Observations of primary tumor tissues before and after castration resistance indicate that AR-V7 expression increases with the outgrowth of CRPC tumors [9, 10]. Abiraterone, a second-generation anti-androgen drug, is approved for CRPC treatment. Resistance to Abiraterone occurs frequently, although it is initially effective for CRPC treatment [11]. Evidence from experimental and clinical studies illustrate that AR-V7 plays a vital role in the promotion and progression of CRPC during ADT and the induction of Abiraterone resistance [12, 13], and in some CRPC patients started with Abiraterone didn't respond, but after several months continuous treatment they could respond to it [12]. However, the mechanism of AR-V7 affecting Abiraterone efficacy and Abiraterone affecting AR-V7 in CRPC treatment is unknown. Notably, noncoding RNA transcripts, such as miRNAs and lncRNAs, play significant roles in the molecular mechanism of cancers [14, 15]. In this study, we first investigated the effect of Abiraterone administration on the AR-V7 expression level of androgen-dependent cell lines *in vitro*. Moreover, AR-V7-related RNAs affecting Abiraterone treatment of CRPC were identified through bioinformatics analysis based on RNA sequencing. Here, we explored the mechanism of Abiraterone effecting AR-V7 and AR-V7 affecting therapy efficacy of Abiraterone, and provide new options for Abiraterone treatment of CRPC.

Methods

Cell culture

The cell lines LNCaP (SCSP-5021, an androgen-dependent PCa cell line), PC-3 (SCSP-532, an androgen-independent cell line lacking AR expression), VCaP (SCSP-5034, a PCa cell line with wild-type AR expression), and 22RV1 (SCSP-5022, CRPC cell line with the expression of AR splice variants) were acquired from the Chinese Academy of Sciences, China. The LNCaP cells were cultured in 90% RPMI-1640 medium (61870127, Gibco, USA) with 10% fetal bovine serum (FBS) (10099141, Gibco, USA) and the VCaP cells were cultured in 90% DMEM (C12571500BT, Gibco, USA) with 10% FBS, 1 mM sodium pyruvate. The 22RV1 cells were cultured in 90% RPMI-1640 medium with 10% FBS, and the PC-3 cells were cultured in 90% F12K nutrient mixture medium (21127-022, Gibco, USA) with 10% FBS. All cell lines were cultured at 37°C with 5% of CO_2 in a humidified atmosphere.

The cell proliferation assay

To assess the effect of Abiraterone on survival, cells were separately treated with 0, 10, 20, 40, 80, 150, 300, or 500 μM Abiraterone (A125745, Aladdin, Shanghai Aladdin Biochemical Technology Co., Ltd). In addition, cell survival was measured using a cell counting kit-8 (CCK-8, Sigma, USA) at 24, 48, or 72 h. The results were detected utilizing a microplate reader (Infinite M100 PRO, TECAN, Switzerland) at a wavelength of 450 nm.

The cell apoptosis assay

The 22RV1 cells (7 ×10^5) and LNCaP cells (2 ×10^5) were treated with 175 μM Abiraterone, and cell proliferation studies were performed at 24, 48 and 72 h using an annexin V-fluorescein isothiocyanate (FITC)-propidium iodide (PI) cell apoptosis kit (Invitrogen, Thermo Fisher Scientific, Inc.). The cells were washed twice with PBS buffer (pH 7.4) then resuspended in the binding buffer. Moreover, 5 μl PI and 5 μl Annexin V-FITC were mixed with the cells. The mixtures were incubated at 25°C for 15 min in the dark, and then the combinations were measured utilizing FACScan flow cytometry (FACSCalibur, BD).

Western blot analysis

Cell samples [untreated cell lines (LNCaP, PC-3, VCaP, and 22RV1), and cell lines (LNCaP and 22RV1) treated for 48 or 72 h with Abiraterone were homogenized in RIPA buffer (P0013B, Biyuntian Biotechnology Co. LTD, China), and a BCA protein kit (PL212989, Thermo, USA) was utilized to detect the protein concentration. Then, 4-12% Sodium dodecylsulphate polyacrylamide gel electrophoresis (SDS-PAGE) was used to separate cell lysates. Subsequently, the extracted proteins were transferred to polyvinylidene difluoride (PVDF) membranes (IPVH00010, Millipore, United States). The PVDF membrane was blocked with 5% skim milk in TBST at 37°C for 2 h, and then incubated with diluted primary rabbit and mouse monoclonal antibodies (1:1,000) overnight at 4°C, containing AR-V7 (ab198394, Abcam) and β-actin (Ab8226, Abcam), and then incubated with the secondary antibody [peroxidase AffiniPure Goat Anti-Rabbit IgG (H+L) (1:10 000, 111-035-045, Jackson] and Peroxidase AffiniPure Donkey Anti-Mouse IgG (H+L) (1: 5,000; 715-035-151, Jackson)] for 2 h at 37°C. The ECL (electro-chemiluminescence) substrate (SB-WB012, Share-bio, China) was used to detect protein bands via a chemiluminescence imaging system (4600, Tanon, China). During this experiment, β-actin was utilized as an internal control.

Real-time quantitative reverse transcription PCR (qRT-PCR)

The total RNA of LNCaP and 22RV1 cells (Abiraterone-treated at 48 or 72 h) was isolated from cell samples utilizing TRIzol (9109, TaKaRa, Japan). After that, 1 μg of the RNA was reverse-transcribed to cDNA. Based on provided protocols (7900HT FAST, ABI, USA), SYBR green-mediated RT-PCR amplification and real-time fluorescence detection were performed. The relative mRNA expression of each gene was normalized to GAPDH. Primers used included: AR-V7 (F):5'-CGGAAATGTTA TGAAGCAGGGATGA-3', AR-V7 (R): 5'-CTGGTCATTTTGAGATGCTTGCAAT-3'; GAPDH (F): 5'-TGACAACTTTGGTATCGTGGAAGG-3', GAPDH (R): 5'-AGGCAGGGATGATGTTCTGGAGAG-3'.

RNA isolation, sequencing, and data preprocessing

Total RNA from 22RV1 cells [a control group (Abiraterone-treated 0 h), the JY-48 h group (Abiraterone-treated for 48 h), and the JY-72 h group (Abiraterone-treated for 72 h), three samples in each group] was extracted as mentioned above. The RNA concentration and purity were performed utilizing a Nanodrop 2000 system (Thermo, USA), and the RNA integrity was electrophoresed onto a 1% agarose gel. Sequencing was performed using an Illumina Hiseq X-ten platform (Illumina, Inc., San Diego, CA, USA). The FASTQ sequence data were acquired from the RNA-sequencing data using Base Calling version 0.11.4. In addition, the FASTQ data quality control was performed utilizing the READ QC tool in FastQC version 0.11.4. Cutadapt version 1.16 was used for raw data trimming. Also, to acquire clean reads, the low-quality reads, including sequences with a quality score < 15, adaptor sequences, and sequences with an N number of raw reads > 1 were removed.

The clean reads were localized to the human reference genome (GENCODE, Homo_GRCh38) using HISAT2 version 2.1.0 [16]. FeatureCounts software version 1.6.0 [17] was used to acquire the read count information mapped on each gene, according to GENCODE [18], which provided human gene annotation information. The “protein-coding” annotation information was used as mRNA, and the annotation information of “antisense,” “sense_intronic,” “sense_overlapping,” “lincRNA,” “processed_transcript,” “bidirectional_promoter_lncRNA,” “non_coding” were used as lncRNA.

Expression level and Pearson correlation coefficient analysis of samples

The cor function in R language was employed to calculate the Pearson correlation coefficient (P) between each pair of samples. The prcomp algorithm in R language was utilized to conduct PCa of samples. Finally, the PCa diagram was performed using the Ggfortify package version 0.4.5.

Differential expression analysis

The voom function in the limma package [19] was employed to standardize the raw counts. The differentially expressed (DE)mRNAs and DE Long non-coding RNAs (lncRNAs) between the JY-48 h group and the control group, or the JY-72 h group and the control group were screened utilizing the limma package with the threshold of adj.$P < 0.05$ and a |log fold change (FC)| > 1. The Benjamini and Hochberg (BH) method was used to adjust the *P*-value for multiple comparisons. In addition, to obtain the AR-V7-related RNAs affecting Abiraterone treatment of CRPC, the DEmRNAs and DElncRNAs screened from the JY-48 h group, and the control group were intersected with DEmRNAs and DElncRNAs screened from the JY72 h group and the control group, and the overlapping DEmRNAs and DElncRNAs were obtained. Then, the overlapping DEmRNAs and DElncRNAs were removed from the DEmRNAs, and DElncRNAs screened from the JY-48 h group and the control group, and the remaining DEmRNAs and DElncRNAs were used for subsequent analyses. Moreover, the featured lncRNAs recorded in the LncBook database [20] were intersected with the other DElncRNAs, and the overlapping lncRNAs were obtained for subsequent analyses.

DEmRNA-DElncRNA co-expression network construction

The P of DEmRNAs and DElncRNAs was calculated based on mRNA and lncRNA data-matched samples. In addition, the BH method was performed to adjust the P values, and the DEmRNAs-DElncRNAs pairs were screened with the cutoff value of r > 0.95 and adj.P < 0.01. Then, the DEmRNA-DElncRNA co-expression networks were constructed utilizing Cytoscape software [21]. Moreover, “prostate cancer” was used as a keyword to search disease-related lncRNAs based on the LncBook database, and the disease-related lncRNAs were marked in the DEmRNA-DElncRNA co-expression networks. Also, “prostate neoplasms, castration-resistant” were used as keywords to search disease-related RNAs based on the CTD database [22] (http://ctdbase.org/) and the GeneCards [23] (https://www.genecards.org/) database, and the disease-related RNAs were marked in the DEmRNA-DElncRNA co-expression networks.

Functional enrichment analysis

Both Gene Ontology (GO), and Kyoto Encyclopedia of Genes and Genomes (KEGG) pathway enrichment analyses were conducted on the target genes of lncRNAs utilizing the Metascape online tool [24] based on the DEmRNAs-DElncRNAs pairs. The parameters were set to min overlap = 3, P = 0.05, min enrichment = 1.5. Based on the mRNAs of the DEmRNAs-DElncRNAs pairs, the DAVID tool [25] was used to perform GO and KEGG pathway enrichment analyses with a cutoff value of P < 0.05 and count ≥ 2.

Protein-protein interaction network building

The Search Tool for the Retrieval of Interacting Genes (STRING) database [26] was performed to analyze the interactions between protein and protein encoded by mRNAs in the DEmRNA-DElncRNA co-expression network. The PPI score was set as 0.4 (referred to as the median confidence). Afterward, the PPI network was built using Cytoscape software. The CytoNCA plugin [27] was used to analyze the degree of nodes in the network, and the parameter was set to “without weight.”

lncRNA-miRNA-mRNA network construction

According to the mRNAs in the DEmRNA-DElncRNA co-expression network, the miRTarBase database [28] was utilized to predict microRNAs (miRNAs), and the miRNA-mRNA pairs were obtained. The DIANA-LncBase database [29] was employed to predict miRNAs based on lncRNAs in the DEmRNA-DElncRNA co-expression network, and the lncRNA-miRNA pairs were obtained. The lncRNA-miRNA-mRNA pairs were further identified according to the positive co-expression relationships between mRNA and lncRNA (r > 0.95), and the competing endogenous RNAs (ceRNA) network was built.

Survival analysis

Based on the lncRNAs and mRNAs in the ceRNA network, the survival analysis was performed utilizing the GEPIA2 online tool [30] (http://gepia2.cancer-pku.cn/#survival), and the statistical significance level was defined as P < 0.05.

Statistical Analysis

The data from each assay were shown as the mean ± standard deviation. One-way analysis of variance (ANOVA), t-tests, and Newman-Keuls multiple comparison tests were performed to assess the statistical significance between groups. All data were analyzed using SPSS 17.0 software and GraphPad Prism. A $P < 0.05$ was regarded as significant.

Results

Abiraterone inhibited cell growth

Drug resistance and sensitivity are conventionally quantified using half-inhibitory concentration values (IC50). To explore the effects of Abiraterone on survival, the cells were separately treated with different concentrations of Abiraterone. As shown in Figure 1A, four cell lines were sensitive to Abiraterone and the inhibition rate increased with increasing Abiraterone concentrations. The IC50 of all cell lines were unchanged at 24 h, while the IC50 of PC-3 and LNCaP cell lines decreased to half of the initial IC50 at 48 h (Figure 1B). The IC50 for LNCaP cells was 344.9 mM. Therefore, half of the LNCaP cell IC50 (172.45 mM) was applied in subsequent experiments.

AR-V7 protein expression in 22RV1 cells is higher than VCaP, LNCaP, or PC-3 cells

AR-V7 has been revealed to be a potential clinical marker for patients with CRPC [31]. To identify the suitable cell line for subsequent analysis, AR-V7 protein expression levels in untreated cell lines (LNCaP, PC-3, VCaP, or 22RV1) were analyzed using western blot analysis. As illustrated in Figure 2, the AR-V7 protein expression level in 22RV1 cells was higher than in VCaP, LNCaP, and PC-3 cells. Therefore, LNCaP and 22RV1 cells were chosen for subsequent analysis because VCaP cells grew slowly.

Abiraterone effectively reduced AR-V7 expression in treated cells

Though some research indicated that AR-V7 status is related to the therapy efficacy of Abiraterone [12, 13], but few papers detected the influence of Abiraterone to AR-V7 expression. In our study, to assess the effect of Abiraterone on AR-V7 expression, qRT-PCR and western blot analyses were conducted. The expression level of AR-V7 mRNA in the Abiraterone-treated 22RV1 cell group was lower than in the control group at 48 h ($P < 0.01$). In comparison, there was no significant difference between the Abiraterone and the control groups at 72 h ($P > 0.05$). AR-V7 mRNA expression in LNCaP cells following Abiraterone treatment was decreased compared with that in the control group at 48 and 72 h ($P < 0.01$) (Figure 3A). In addition, the results of western blot analysis further indicated that Abiraterone administration reduced AR-V7 expression levels (Figure 3B).

Abiraterone resistance in 22RV1 cells 48 and 72 h post-treatment

As shown in Figure 4A, the results showed that cell apoptosis significantly increased in 22RV1 cells following 24 h Abiraterone treatment ($P < 0.01$), while the Abiraterone group and the control group

showed no significant differences ($P > 0.05$) after 48 or 72 h. The proportion of apoptotic LNCaP cells in the Abiraterone group was significantly increased compared with that in the control group at 24, 48, and 72 h ($P < 0.01$) (Figure 4B). The results revealed that resistance to Abiraterone occurred in 22RV1 cells at 48 and 72 h, although Abiraterone is effective at 24 h. Thus, 22RV1 cells were used for RNA-sequencing.

Expression level analysis and PCA of samples

After quality control and filtering, a total of 24,043 RNAs, including 16,457 mRNAs and 7,586 lncRNAs, were identified in 22RV1 cells. The cor function in R language was employed to calculate the Pearson correlation coefficient (P) between each pair of samples. The correlation heatmap of each pair of samples is shown in Figure 5A. In addition, the control, JY-48 h, and JY-72 h samples were entirely separated, meaning that the expression patterns of these samples could be used to ultimately distinguish between the control, JY-48 h, and JY-72 h groups (Figure 5B).

Identification of DEmRNAs and DElncRNAs

Following the application of the thresholds of adj.$P < 0.05$ and |log fold change (FC)| > 1, a total of 1,964 DEmRNAs (of which 686 and 1,278 were up- and downregulated, respectively) and 664 DElncRNAs (of which 222 and 442 were up- and downregulated, respectively) were screened between the control and JY-48 h groups. A total of 4,344 DEmRNAs (of which 2,679 and 1,665 were up- and downregulated, respectively) and 1,483 DElncRNAs (of which 818 and 665 were up- and downregulated, respectively) were compared between the control and JY-72 h groups. In addition, to identify the AR-V7-related RNAs, the 989 DEmRNAs and 398 DElncRNAs were used for subsequent analysis (Figures 6 A and B, Supplementary file 1). Hierarchical clustering analysis of the 989 DEmRNAs and 398 DElncRNAs is shown in Figures 6 C and D.

The DEmRNA-DElncRNA co-expression network

A total of 627 DEmRNA-DElncRNA co-expression pairs were identified with the cutoff value of r > 0.95 and adj.$P < 0.01$, containing 22 DElncRNAs and 389 DEmRNAs. The DEmRNA-DElncRNA co-expression network was constructed utilizing Cytoscape software (Figure 7) and the disease-related RNAs were marked in the DEmRNA-DElncRNA co-expression networks. The results showed that the lncRNAs PRNCR1 and CTB-89H12.4, and the telomerase RNA component (TERC) were related to CRPC.

Functional enrichment analyses of lncRNA target genes and mRNAs

To further elucidate the functional role of the DElncRNAs and DEmRNAs in CRPC, we used the Metascape online tool and the DAVID tool to perform functional enrichment and KEGG pathway analyses of the target genes of lncRNAs and DEmRNAs. Responses to hypoxia, decreased oxygen levels, and oxygen levels were significantly enriched GO terms of the DElncRNAs target genes (Figure 8A). The ErbB signaling pathway (hsa04012), pathways in cancer (hsa05200), and endocrine resistance (hsa01522) were the primary enriched KEGG pathways of DElncRNA target genes (Figure 8B). The upregulated DEmRNAs were mainly enriched in 4 GO terms [including lactation, protein autophosphorylation, protein

phosphorylation, and embryonic pattern specification] and the 0 KEGG pathway (Figure 8C). In addition, the downregulated DEmRNAs were mainly involved in 27 GO terms and 2 KEGG pathways (hsa04012: ErbB signaling pathway, hsa05217: Basal cell carcinoma) (Figure 8D).

PPI network construction

To analyze the interactions between protein and protein encoded by mRNAs in the DEmRNA-DElncRNA co-expression network, the PPI network was built. In total, 379 PPI pairs were acquired from the PPI network (Figure 9). In this PPI network, the notch receptor 1 (NOTCH1), the ionotropic NMDA glutamate receptor type subunit 1 (GRIN1), U-box containing protein 1 (STUB1), and mitogen-activated protein kinase 7 (MAP2K7) with high degrees from a local network and may be the key proteins in the development of CRPC (Supplementary file 2). In addition, the results showed that NOTCH1, STUB1, and the CCAAT enhancer-binding protein alpha (CEBPA) were related to CRPC.

lncRNA-miRNA-mRNA network construction

In total, 6,490 miRNA-mRNA and 5,728 lncRNA-miRNA pairs were obtained. Moreover, 1,702 lncRNA-miRNA-mRNA pairs were screened with the threshold of $r > 0.95$. The miRNAs of lncRNA-miRNA-mRNA pairs with a connectivity ≥ 5 were used to build the ceRNA network. Finally, 479 lncRNA-miRNA-mRNA pairs were used to construct the ceRNA network, including 440 miRNA-mRNA pairs, 209 lncRNA-miRNA pairs, and 127 lncRNA-mRNA pairs (Figure 10). Here, MAP2K7 was regulated by hsa-miR-6825-5p, which was in turn regulated by the lncRNA MAFG-AS1.

Survival analysis

To screen the RNAs that could be potentially used as prognostic biomarkers of CRPC, survival analysis was performed utilizing the GEPIA2 online tool. A total of 4 lncRNAs (CTB-89H12.4, LINC00612, MAFG-AS1, and SLC16A1-AS1) and 17 mRNAs (B4GALNT4, CTU1, GRINA, HLX, LAMC3, MBNL2, NR2F6, ODF2L, PRRC2A, RHOF, RNF126, RSRP1, RTN4R, SLC2A4RG, TOR4A, ZNF467, and ZNF865) were associated with disease-free survival (RFS) (Supplementary file 3). Among them, only MBNL2 overexpression revealed good survival outcomes. The results of lncRNA MAFG-AS1 and MBNL2 are shown in Figure 11.

Discussion

Previous studies have established that AR-V7 plays critical roles in the progression of CRPC. For instance, Chen et al. suggested that HoxB13 might serve as a therapeutic target for AR-V7-driven prostate tumor treatment [32]. Scher et al. validated that nuclear expression of AR-V7 protein in circulating tumor cells in men with metastatic CRPC could serve as a treatment-specific biomarker [6]. However, the regulatory mechanism of AR-V7 affecting Abiraterone treatment of CRPC is unknown. In this study, we found that Abiraterone administration significantly reduced AR-V7 expression levels *in vitro*, this may explain why some CRPC patients started with Abiraterone didn't respond, but after several months continuous treatment they could respond to it for AR-V7 expression is reduced by lone term Abiraterone treatment.

Therefore, AR-V7-related RNAs affecting Abiraterone treatment of CRPC were identified using bioinformatics analysis. The target genes of DEmRNAs and DElncRNAs were primarily involved in cancer-related pathways, including the ErbB signaling pathway, pathways in cancer, and basal cell carcinoma. In addition, NOTCH1, GRIN1, STUB1, and MAP2K7 were found with high degree in the PPI network. Moreover, MAP2K7 was regulated by hsa-miR-6825-5p, and hsa-miR-6825-5p was regulated by lncRNA MAFG-AS1 in the ceRNA network. The survival analysis showed that a total of four lncRNAs (including MAFG-AS1) and 17 mRNAs (including MBNL2) were associated with RFS. Among them, only MBNL2 overexpression correlated with a good survival outcome.

The Notch family of receptors determines the fate of cells in many organ systems, including the prostate [33]. Rice et al. have suggested that the loss of NOTCH1 in aggressive PCa cells decreases proliferation, invasion, and tumorsphere formation [34]. Kwon et al. shown that Notch1 promotes cell survival and proliferation in rat luminal prostate cells through the activation of the pro-survival NF-κB pathway [35]. STUB1 is a type of accessory chaperone protein and an E3 ubiquitin ligase. STUB1 connects the polypeptide binding activity of HSP70 to the ubiquitin-proteasome system. Liu et al. considered that inhibiting the HSP70 targeting protease stabilization pathway may be a valuable strategy for overcoming anti androgen resistance in the next generation of CRPC patients [36].

Nevertheless, the role of GRIN1 in PCa development has not been explored. Herein, NOTCH1, GRIN1, STUB1 exhibited high degrees in the PPI network, and the survival analysis showed that MBNL2 overexpression revealed a good survival outcome. Bii et al. illustrated that MBNL2 was identified as a candidate gene in PCa progression [37]. Zhu et al. demonstrated that miR-636 promotes cell invasion and migration, which might promote bone metastasis of PCa by targeting MBNL2 [38]. Taken together, we speculate that NOTCH1, GRIN1, STUB1, and MBNL2 contribute to the progression of CRPC.

The lncRNA MAFG-AS1 is reportedly related to the progression of cancer. For instance, MAFG-AS1 lncRNA is considered a novel oncogenic lncRNA in the progression of colorectal cancer through its regulation of miR-147b/NDUFA4 [39]. Jia et al. demonstrated that overexpression of MAFG-AS1 lncRNA primarily downregulated miR-339-5p levels in non-small-cell carcinoma cells, and MMP15 is a miR-339-5p target [40]. In addition, Hu et al. illustrated that MAP2K7 might be a promising prognostic molecular biomarker in PCa [41]. Nevertheless, the role of hsa-miR-6825-5p in PCa development has not been explored. Moreover, Wang et al. implied that N-cadherin promotes cancer stem cell-like traits and epithelial-mesenchymal transition through the ErbB signaling pathway in PCa cells [42]. In this study, MAP2K7 was regulated by hsa-miR-6825-5p, and hsa-miR-6825-5p was regulated by MAFG-AS1 lncRNA in the ceRNA network. Moreover, the enrichment analysis found that MAP2K7 is involved in the ErbB signaling pathway. Altogether, this study revealed that the MAFG-AS1-hsa-miR-6825-5p-MAP2K7 axis could be related to the progression of CRPC treatment.

Although we explored the potential molecular mechanisms of Abiraterone treatment in CRPC occurrence and development using a bioinformatics approach, there still exist some limitations in our study. For

instance, relevant experiments, including cell biology assays, and animal and clinical studies need to be performed to verify the multiple target candidates and signaling pathways identified by our bioinformatics analyses.

Conclusions

In summary, NOTCH1, GRIN1, STUB1, MBNL2, and the ErbB signaling pathway were likely related to the progression of CRPC treatment. Moreover, the MAFG-AS1-hsa-miR-6825-5p-MAP2K7 axis might be a therapeutic target for Abiraterone in CRPC treatment. This study may provide new strategies for further studies of Abiraterone in CRPC treatment.

Abbreviations

AR-V7: androgen receptor variant 7;

CRPC: castration-resistant prostate cancer;

qRT-PCR: quantitative reverse transcription PCR;

lncRNAs: long non-coding RNAs;

DE: differentially expressed;

PPI: protein-protein interaction;

ceRNA: competing endogenous RNAs;

NOTCH1: notch receptor 1;

STUB1: U-box containing protein 1;

MAP2K7: mitogen-activated protein kinase;

MBNL2: muscle blind like splicing regulator 2;

RFS: disease-free survival;

Prostate Cancer: PCa;

miRNA: mircro-RNAs;

ADT: androgen deprivation therapy;

PSA: prostate specific antigen;

AR: androgen receptor;

AR-Vs: AR splice variants;

FITC: annexin V-fluorescein isothiocyanate;

PI: propidium iodide;

SDS-PAGE: Sodium dodecylsulphate polyacrylamide gel electrophoresis;

PVDF: polyvinylidene difluoride;

GO: gene ontology;

KEGG: Kyoto encyclopedia of genes and genomes;

STRING: search tool for the retrieval of interacting genes;

ANOVA: one-way analysis of variance;

GRIN1: ionotropic NMDA glutamate receptor type subunit 1;

CEBPA: CCAAT enhancer-binding protein alpha;

Declarations

Ethics approval and consent to participate:

Not applicate, this research did not include in vivo and human experiment, so Ethics approval and consent to participate is not included.

Consent for publication:

Written informed consent for publication was obtained from all participants;

Availability of data and material:

All experiment were finished in our Lab, all data used in this article are promising true and available, anyone who is interested in this research can contact me by E-mail: dupeng9000@126.com, I can sent the original data by E-mail;

Competing interests:

All authors declared no competing interests;

Funding:

The research was financially supported by The Capital Clinical Characteristics Application Research.

Author's contributions:

PD and SW designed this study; SW, YDC , XXT, PD and YY performed the experiments and analyzed the data; SW, YDC, XXT, PD wrote and revised the manuscript; SW, YDC, XXT contributed the same in this article as the first-Cor author.

Acknowledgements:

Our deepest gratitude goes to the editors and anonymous reviewers for your careful work and thoughtful suggestions that have helped improve this paper substantially.

References

1. Bray, F., et al., Global cancer statistics 2018: GLOBOCAN estimates of incidence and mortality worldwide for 36 cancers in 185 countries. CA Cancer J Clin, 2018. 68(6): p. 394-424.
2. Wei, Y., et al., Current Treatment for Low-Risk Prostate Cancer in China: A National Network Survey. J Cancer, 2019. 10(6): p. 1496-1502.
3. Chandrasekar, T., et al., Mechanisms of resistance in castration-resistant prostate cancer (CRPC). Transl Androl Urol, 2015. 4(3): p. 365-80.
4. Attard, G., J. Richards, and J.S. de Bono, New strategies in metastatic prostate cancer: targeting the androgen receptor signaling pathway. Clin Cancer Res, 2011. 17(7): p. 1649-57.
5. Sieuwerts, A.M., et al., AR splice variants in circulating tumor cells of patients with castration-resistant prostate cancer: relation with outcome to cabazitaxel. Mol Oncol, 2019. 13(8): p. 1795-1807.
6. Scher, H.I., et al., Association of AR-V7 on Circulating Tumor Cells as a Treatment-Specific Biomarker With Outcomes and Survival in Castration-Resistant Prostate Cancer. JAMA Oncol, 2016. 2(11): p. 1441-1449.
7. Kallio, H.M.L., et al., Constitutively active androgen receptor splice variants AR-V3, AR-V7 and AR-V9 are co-expressed in castration-resistant prostate cancer metastases. Br J Cancer, 2018. 119(3): p. 347-356.
8. Zhu, Y., et al., Novel Junction-specific and Quantifiable In Situ Detection of AR-V7 and its Clinical Correlates in Metastatic Castration-resistant Prostate Cancer. Eur Urol, 2018. 73(5): p. 727-735.
9. Lokhandwala, P.M., et al., Analytical Validation of Androgen Receptor Splice Variant 7 Detection in a Clinical Laboratory Improvement Amendments (CLIA) Laboratory Setting. J Mol Diagn, 2017. 19(1): p. 115-125.
10. Del Re, M., et al., The Detection of Androgen Receptor Splice Variant 7 in Plasma-derived Exosomal RNA Strongly Predicts Resistance to Hormonal Therapy in Metastatic Prostate Cancer Patients. Eur Urol, 2017. 71(4): p. 680-687.

11. Antonarakis, E.S., et al., AR-V7 and resistance to enzalutamide and Abiraterone in prostate cancer. N Engl J Med, 2014. 371(11): p. 1028-38.
12. Sarwar, M., et al., Targeted suppression of AR-V7 using PIP5K1α inhibitor overcomes enzalutamide resistance in prostate cancer cells. Oncotarget, 2016. 7(39): p. 63065-63081.
13. Chung, J.S., et al., Circulating Tumor Cell-Based Molecular Classifier for Predicting Resistance to Abiraterone and Enzalutamide in Metastatic Castration-Resistant Prostate Cancer. Neoplasia, 2019. 21(8): p. 802-809.
14. Qadir, M.I. and A. Faheem, miRNA: A Diagnostic and Therapeutic Tool for Pancreatic Cancer. Crit Rev Eukaryot Gene Expr, 2017. 27(3): p. 197-204.
15. Bhan, A., M. Soleimani, and S.S. Mandal, Long Noncoding RNA and Cancer: A New Paradigm. Cancer Res, 2017. 77(15): p. 3965-3981.
16. Kim, D., B. Langmead, and S.L. Salzberg, HISAT: a fast spliced aligner with low memory requirements. Nat Methods, 2015. 12(4): p. 357-60.
17. Liao, Y., G.K. Smyth, and W. Shi, featureCounts: an efficient general purpose program for assigning sequence reads to genomic features. Bioinformatics, 2014. 30(7): p. 923-30.
18. Frankish, A., et al., GENCODE reference annotation for the human and mouse genomes. Nucleic Acids Res, 2019. 47(D1): p. D766-d773.
19. Smyth, G.K., limma: Linear Models for Microarray Data. 2013.
20. Lina, M., et al., LncBook: a curated knowledgebase of human long non-coding RNAs. Nucleic Acids Research, 2019(5): p. 5.
21. Shannon, P., et al., Cytoscape: a software environment for integrated models of biomolecular interaction networks. Genome Res, 2003. 13(11): p. 2498-504.
22. Davis, A.P., et al., The Comparative Toxicogenomics Database: update 2019. Nucleic Acids Res, 2019. 47(D1): p. D948-d954.
23. Stelzer, G., et al., The GeneCards Suite: From Gene Data Mining to Disease Genome Sequence Analyses. Curr Protoc Bioinformatics, 2016. 54: p. 1.30.1-1.30.33.
24. Zhou, Y., et al., Metascape provides a biologist-oriented resource for the analysis of systems-level datasets. Nat Commun, 2019. 10(1): p. 1523.
25. Huang da, W., B.T. Sherman, and R.A. Lempicki, Systematic and integrative analysis of large gene lists using DAVID bioinformatics resources. Nat Protoc, 2009. 4(1): p. 44-57.
26. Szklarczyk, D., et al., STRING v10: protein-protein interaction networks, integrated over the tree of life. Nucleic Acids Res, 2015. 43(Database issue): p. D447-52.
27. Tang, Y., et al., CytoNCA: a cytoscape plugin for centrality analysis and evaluation of protein interaction networks. Biosystems, 2015. 127: p. 67-72.
28. Chou, C.H., et al., miRTarBase update 2018: a resource for experimentally validated microRNA-target interactions. Nucleic Acids Res, 2018. 46(D1): p. D296-d302.

29. Paraskevopoulou, M.D., et al., DIANA-LncBase v2: indexing microRNA targets on non-coding transcripts. Nucleic Acids Res, 2016. 44(D1): p. D231-8.
30. Tang, Z., et al., GEPIA2: an enhanced web server for large-scale expression profiling and interactive analysis. Nucleic Acids Res, 2019. 47(W1): p. W556-w560.
31. Sciarra, A., et al., Androgen receptor variant 7 (AR-V7) in sequencing therapeutic agents for castratrion resistant prostate cancer: A critical review. Medicine (Baltimore), 2019. 98(19): p. e15608.
32. Chen, Z., et al., Diverse AR-V7 cistromes in castration-resistant prostate cancer are governed by HoxB13. Proc Natl Acad Sci U S A, 2018. 115(26): p. 6810-6815.
33. Stoyanova, T., et al., Activation of Notch1 synergizes with multiple pathways in promoting castration-resistant prostate cancer. Proc Natl Acad Sci U S A, 2016. 113(42): p. E6457-e6466.
34. Rice, M.A., et al., Loss of Notch1 Activity Inhibits Prostate Cancer Growth and Metastasis and Sensitizes Prostate Cancer Cells to Antiandrogen Therapies. Mol Cancer Ther, 2019. 18(7): p. 1230-1242.
35. Kwon, O.J., et al., Increased Notch signalling inhibits anoikis and stimulates proliferation of prostate luminal epithelial cells. Nat Commun, 2014. 5: p. 4416.
36. Liu, C., et al., Proteostasis by STUB1/HSP70 complex controls sensitivity to androgen receptor targeted therapy in advanced prostate cancer. Nat Commun, 2018. 9(1): p. 4700.
37. Bii, V.M., et al., Replication-incompetent gammaretroviral and lentiviral vector-based insertional mutagenesis screens identify prostate cancer progression genes. Oncotarget, 2018. 9(21): p. 15451-15463.
38. Zhu, Z., et al., Identifying the key genes and microRNAs in prostate cancer bone metastasis by bioinformatics analysis. FEBS Open Bio, 2020. 10(4): p. 674-688.
39. Cui, S., et al., LncRNA MAFG-AS1 promotes the progression of colorectal cancer by sponging miR-147b and activation of NDUFA4. Biochem Biophys Res Commun, 2018. 506(1): p. 251-258.
40. Jia, Y.C., et al., LncRNA MAFG-AS1 facilitates the migration and invasion of NSCLC cell via sponging miR-339-5p from MMP15. Cell Biol Int, 2019. 43(4): p. 384-393.
41. Hu, D., et al., Development of an autophagy-related gene expression signature for prognosis prediction in prostate cancer patients. J Transl Med, 2020. 18(1): p. 160.
42. Wang, M., et al., N-cadherin promotes epithelial-mesenchymal transition and cancer stem cell-like traits via ErbB signaling in prostate cancer cells. Int J Oncol, 2016. 48(2): p. 595-606.

Figures

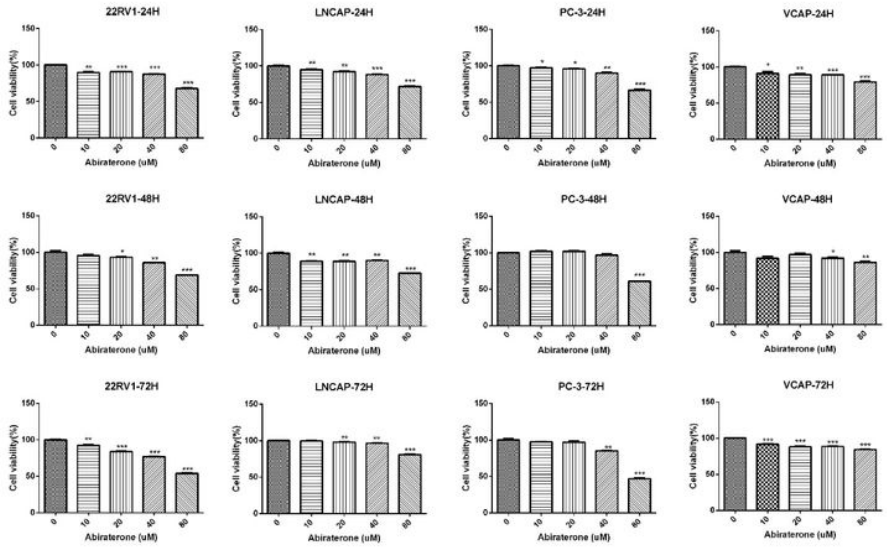

1A

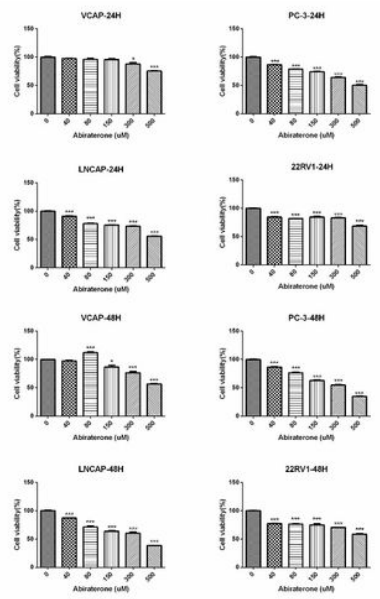

1B

Figure 1

Abiraterone inhibited cell growth Abiraterone resistance and sensitivity are conventionally quantified by the half-inhibitory concentration (IC50). (A) The inhibition rate of cells treated with Abiraterone. LNCaP, PC-3, VCaP, and 22RV1 cells were separately treated with 0, 10, 20, 40, or 80 μM Abiraterone. The survival observations were measured using the cell counting kit-8 (CCK-8) according to the manufacturer's protocol at 24, 48, or 72 h. (B) The inhibition rate of cells treated with Abiraterone. The LNCaP, PC-3, VCaP, and 22RV1 cells were separately treated with 0, 40, 80, 150, 300, or 500 μM Abiraterone. The survival observations were measured using the cell counting kit-8 (CCK-8) according to the manufacturer's protocol at 24 and 48 h. The results are shown as the mean ± standard deviation. *P < 0.05, **P < 0.01, ***P < 0.0001 versus the 0 μM group.

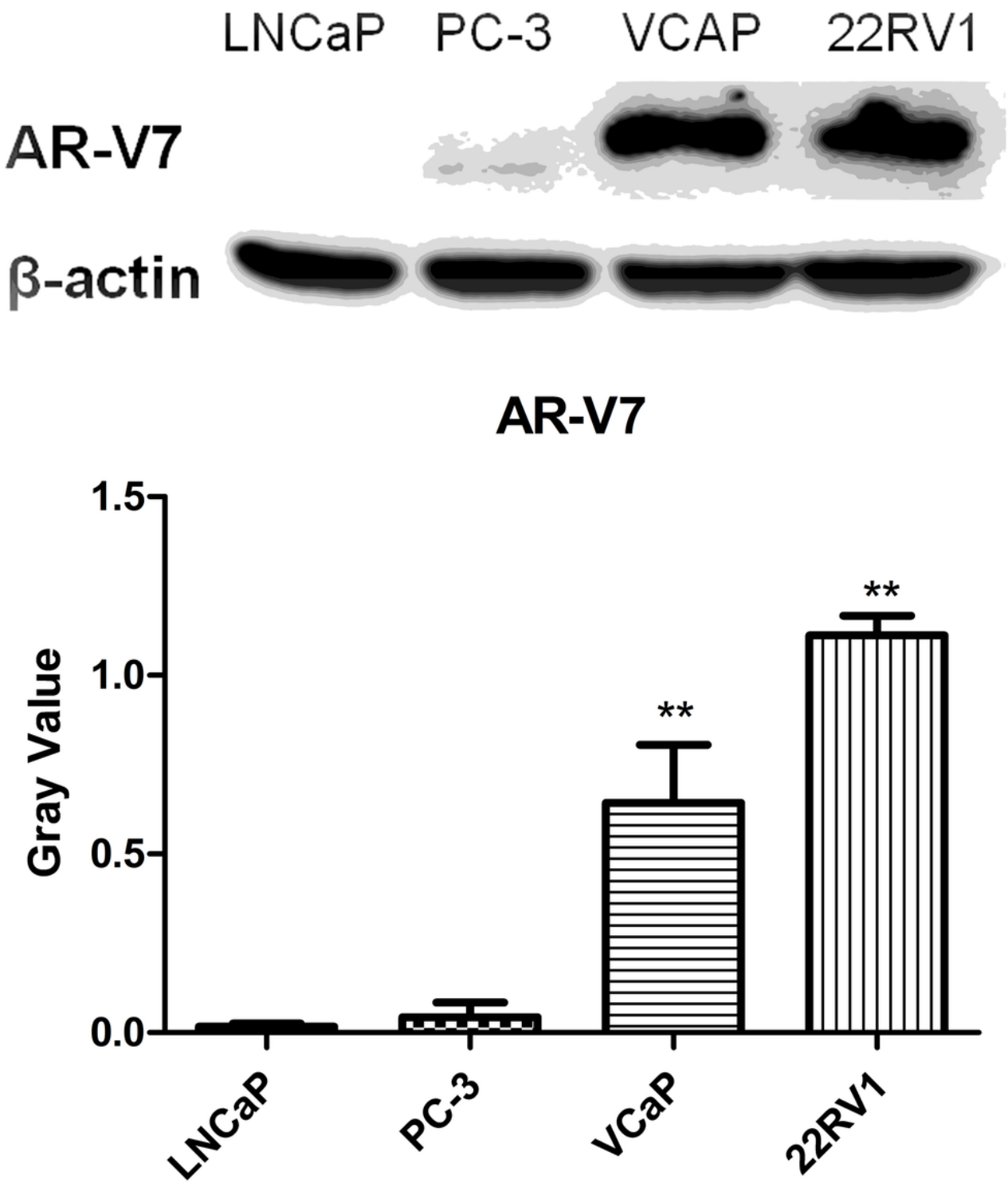

Figure 2

AR-V7 protein expression in 22RV1 cells is higher than VCaP, LNCaP, and PC-3 cells AR-V7 protein expression in untreated cell lines (LNCaP, PC-3, VCaP, and 22RV1) was analyzed utilizing western blot analysis, and β-actin was used as an internal control. Results are shown as the mean ± standard deviation. **P < 0.01 versus the LNCaP group.

Figure 3

Abiraterone effectively reduced AR-V7 expression in Abiraterone-treated cells. To assess the effects of Abiraterone on AR-V7 expression, western blot analysis, and real-time quantitative reverse transcription PCR (qRT-PCR) were performed. (A) The qRT-PCR results of Abiraterone treatment on AR-V7 expression at 48 and 72 h. (B) Western blot analysis results showing the effects of Abiraterone treatment on AR-V7 expression at 48 and 72 h. Results are shown as the mean ± standard deviation. *P < 0.05, **P < 0.01 versus the control group.

Figure 4

Abiraterone resistance in 22RV1 cells 48 and 72 h after treatment An annexin V-fluorescein isothiocyanate (FITC)/ propidium iodide (PI) cell apoptosis kit was used to analyze the cell apoptosis following 24, 48 or 72 hr treatment with Abiraterone. (A) Cell apoptosis in 22RV1 cells; (B) Cell apoptosis in LNCaP cells. Results are shown as the mean ± standard deviation. **P < 0.01 versus the LNCaP group.

Figure 5

Expression level analysis and principal component analysis (PCA) of samples (A) The correlation coefficient between different samples; (B) Principal component analysis was used to evaluate the grouping of samples.

Figure 6

DEmRNAs and DElncRNAs compared between the control and JY-48 h groups, and the control and JY-72 h groups (A) The Venn diagram of DEmRNAs; (B) The Venn diagram of DElncRNAs; (C) Hierarchical clustering results of 989 DEmRNAs; (D) Hierarchical clustering results of 398 DElncRNAs. DElncRNAs, differentially expressed lncRNAs; DEmRNAs, differentially expressed mRNAs

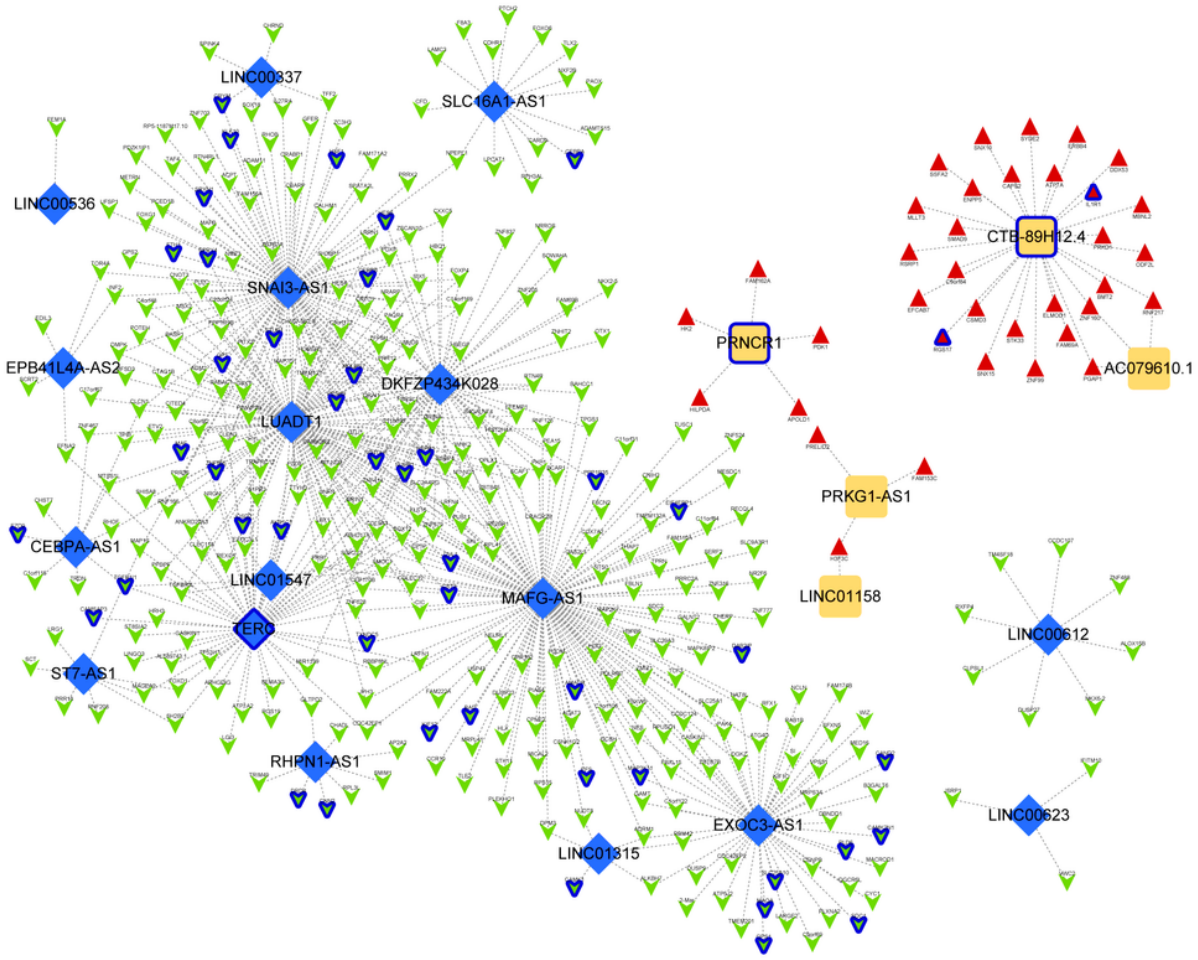

Figure 7

The DEmRNA-DElncRNA co-expression network Green inverted triangles represent downregulated mRNAs; red triangles represent upregulated mRNAs; blue rhomboids represent downregulated lncRNAs; yellow squares represent upregulated lncRNAs; nodes with dark blue outer rims represent drug-related genes.

Figure 8

Enrichment analyses of lncRNAs and mRNAs (A) GO terms and (B) KEGG pathways for DElncRNA target genes; (C) GO terms for upregulated DEmRNAs; (D) GO terms and KEGG pathways for downregulated DEmRNA target genes. The size of the ball represents the number of genes enriched in each term. The color of the ball represents the p-value. DElncRNAs, differentially expressed lncRNAs; DEmRNAs, differentially expressed mRNAs; GO: Gene Ontology; KEGG: Kyoto Encyclopedia of Genes and Genomes

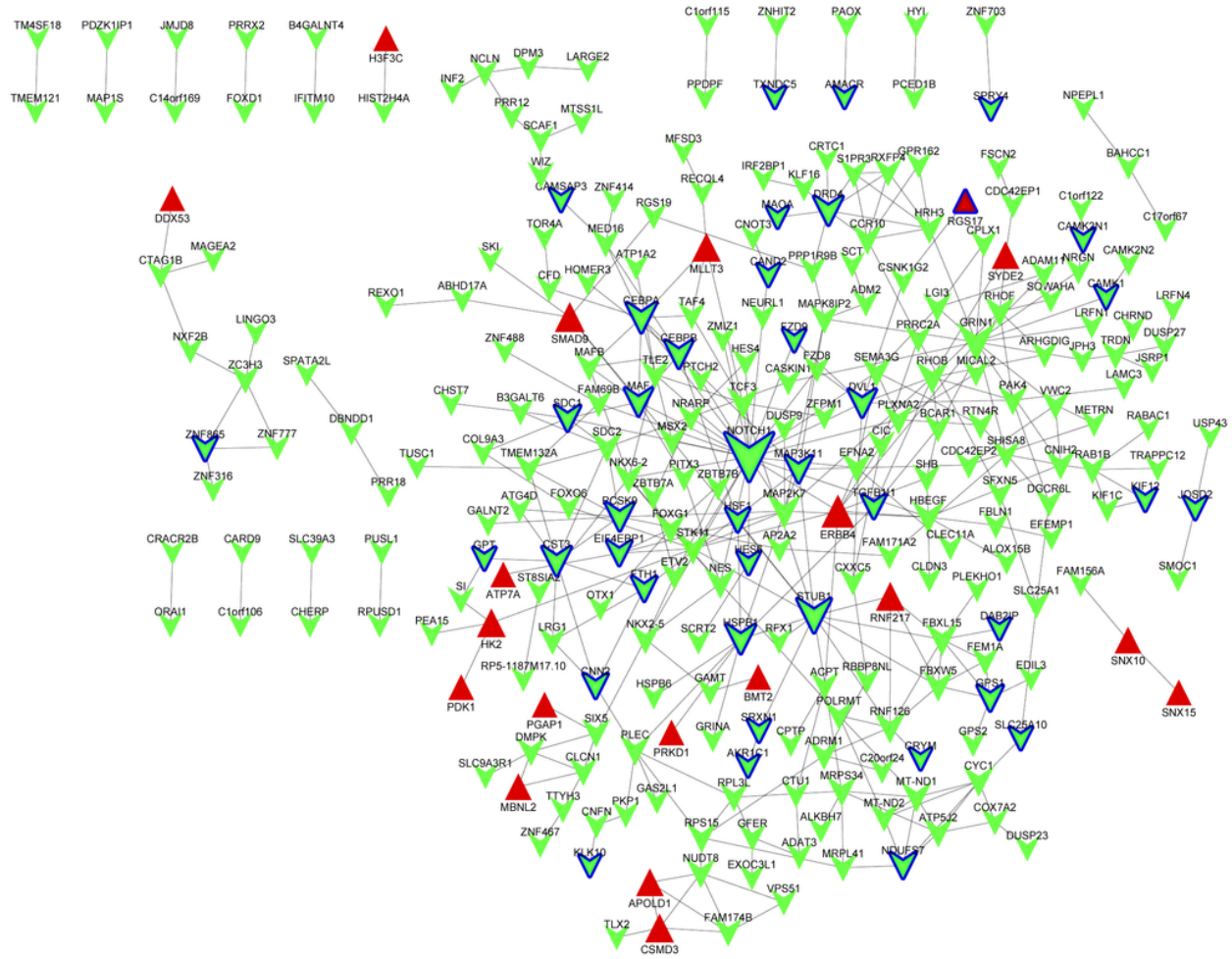

Figure 9

PPI network analysis Green inverted triangles represent downregulated protein; red triangles represent upregulated protein; modes with dark blue outer rims represent drug-related proteins. PPI: protein-protein interaction

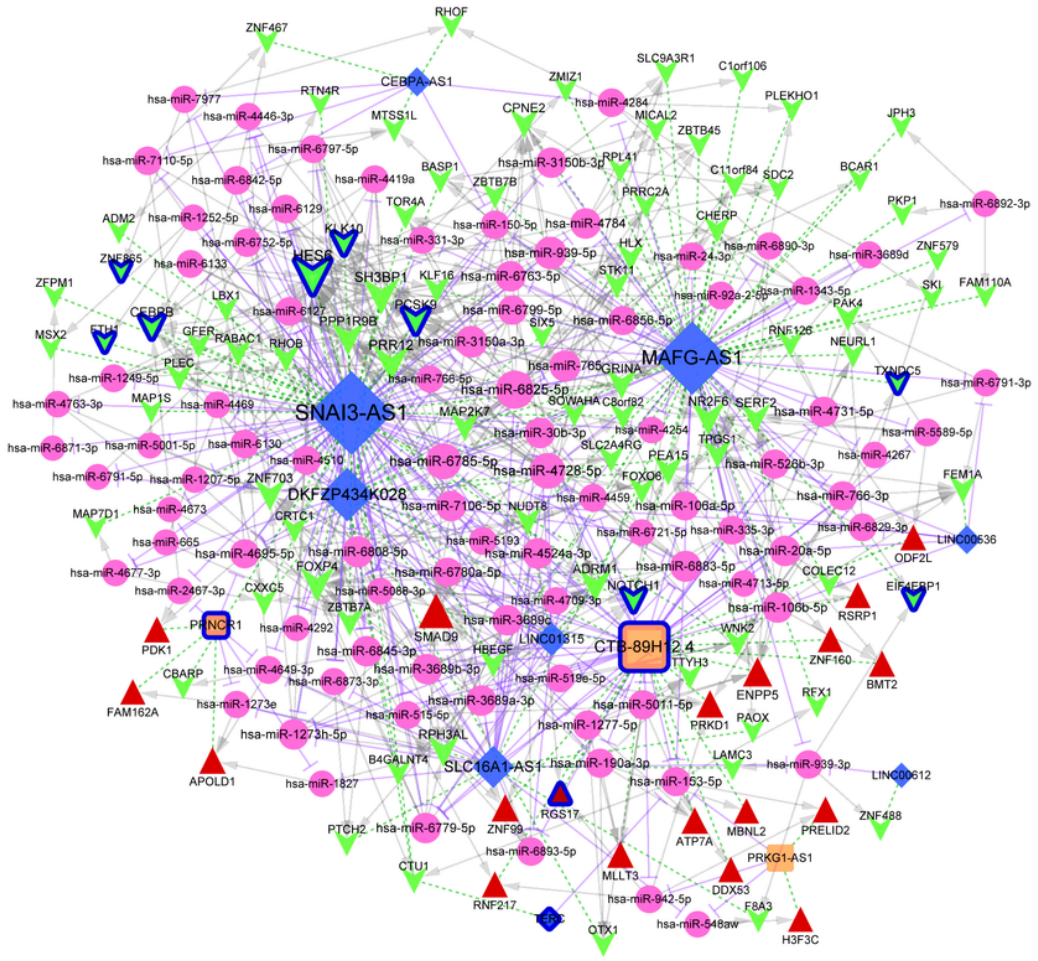

Figure 10

lncRNA-miRNA-mRNA network construction Green inverted triangles represent downregulated mRNA; red triangles represent upregulated mRNA; yellow squares represent upregulated lncRNA; blue rhomboids represent downregulated lncRNA; pink nodes represent miRNA; nodes with dark blue outer rims represent drug-related proteins; Gray arrow lines represent miRNA-mRNA regulatory relationships; purple T lines represent lncRNA-miRNA regulatory relationships; green-dotted lines represent lncRNA-mRNA regulatory relationships; the size of nodes represents its degree.

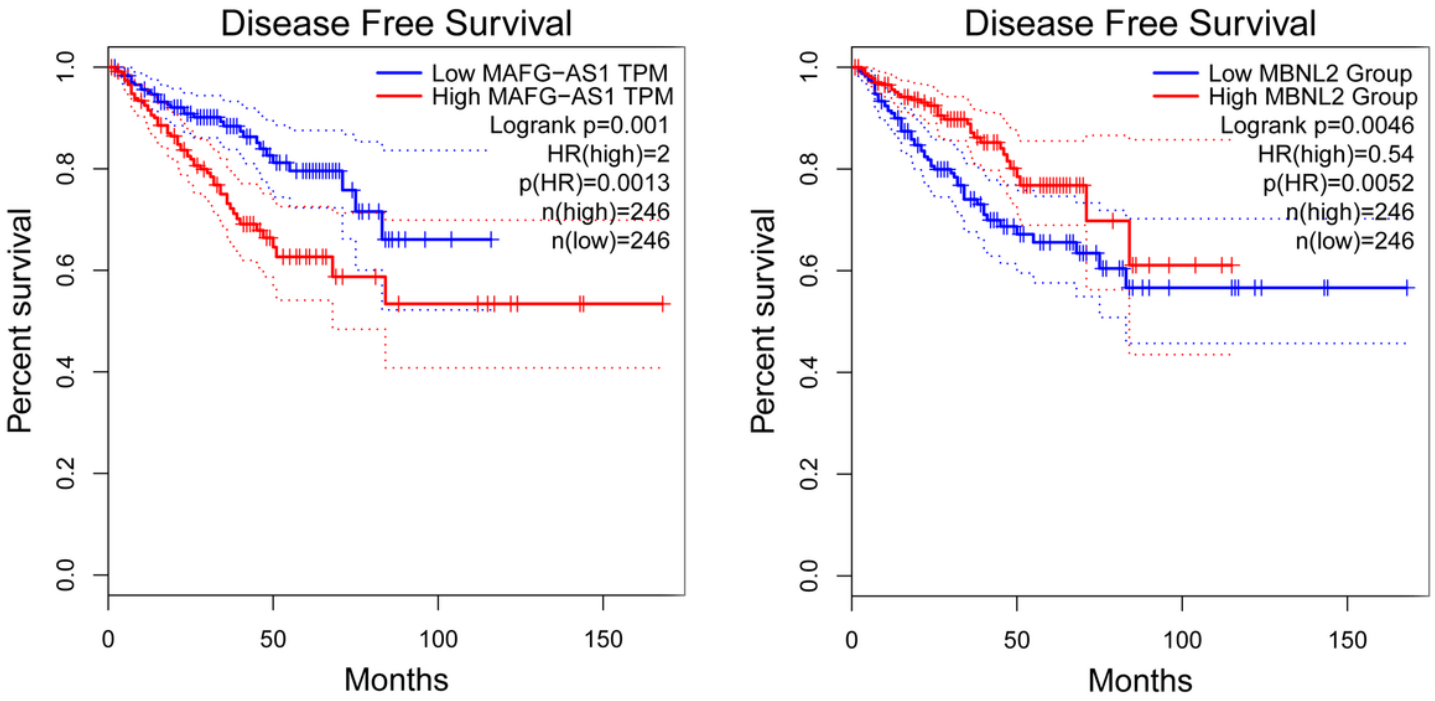

Figure 11

Survival analysis results of lncRNA MAFG-AS1 and MBNL2

Supplementary Files

This is a list of supplementary files associated with this preprint. Click to download.

- additionfilesoriginalblotimage.docx